

Structure and Stability of the Organo-Noble Gas Molecules XNgCCX and XNgCCNgX (Ng = Kr, Ar; X = F, Cl)[†]

Scott Yockel, Evan Gawlik, and Angela K. Wilson*

Center for Advanced Scientific Computing and Modeling, Department of Chemistry, University of North Texas, Box 305070, Denton, Texas 76203-5070

Received: February 13, 2007; In Final Form: July 3, 2007

Density functional theory (B3LYP) and ab initio theory [second-order Møller–Plesset perturbation theory (MP2) and coupled-cluster theory including single, double, and quasiperturbative triple excitations (CCSD(T))] have been used in combination with the standard and augmented correlation consistent basis sets (cc-pVnZ and aug-cc-pVnZ, where n = D, T, and Q) to investigate potential new noble gas compounds. Two classes of molecules were studied: XNgCCNgX and XNgCCX, where Ng = Kr and Ar and X = F and Cl. These molecules were characterized by finding the ground-state structures and calculating the relative energies, charge distributions, and vibrational frequencies. In addition, transition-state structures were also determined and decomposition pathways were identified through intrinsic reaction coordinate calculations.

I. Introduction

Originally, the noble gases were widely believed to be incapable of chemical bonding to other atoms. Pauling first suggested the possibility of noble gases forming chemical bonds with other atoms in 1933,¹ but his hypothesis remained unconfirmed for nearly three decades. Bartlett's synthesis of XePtF₆ marked the beginning of a new era in noble gas chemistry.² More recently, a small number of molecules containing bonds with noble gases (argon, krypton, or xenon) have been synthesized and observed experimentally and have been predicted computationally. Among the most common are linear triatomic molecules of the form HNgX, where Ng is a noble gas atom and X is a halogen.^{3–16} These initial studies^{9–12,17,18} have helped to understand the level of theory (the sophistication of the method and the flexibility of the basis set) needed to predict chemical properties, such as minimum energy and transition state structures as well as dissociation pathways and other energetic properties, of these noble gas bonded systems.

Recent work has suggested noble gas atom insertion into hydrocarbons, yielding a new class of molecules appropriately named “organo-noble gas” compounds. Lundell et al. provided the first such study, in which MP2 and CCSD(T) computations were used to predict structures where Xe had been inserted into C–H and O–H bonds to form HXeCCH, HXeC₆H₅, and HXeOC₆H₅.¹⁹ Shortly thereafter, Feldman and co-workers²⁰ and the Räsänen group²¹ reported the experimental synthesis of HXeCCH using a matrix isolation technique, whereby they photolyzed HCCH creating H and CCH radicals which bonded with xenon. In addition, the Räsänen group detected the formation of HXeCC and HXeCCXeH with infrared spectroscopy.²¹ Both of these species also had been studied by Lundell et al. using computational methods. In the current study, it is envisioned that a similar synthesis strategy could be used to make FKrCCF and other derivatives by photolysis of FCCF. There are a few prior studies that have characterized the

vibrational and rotational spectra of FCCF;^{22–24} however, much less is known about the photochemistry of FCCF in comparison to HCCH.

Räsänen's work marked the first time a neutral noble gas hydride that contained two xenon atoms had been synthesized. The analogous krypton species HKrCCH was then synthesized by the Räsänen group, providing the first “organo-krypton” system. However, HKrCC and HKrCCKrH were not believed to have been formed during the synthesis of HKrCCH, since no vibrational bands were observed for these additional species.²⁵ The Räsänen group also performed theoretical computations that provided a possible reason for the absence of the HKrCC and HKrCCKrH molecules in the experimental infrared analysis. From their all-electron correlated MP2 computations with the aug-cc-pVDZ basis set, HKrCC was found to be 1.38 eV higher in energy than H + Kr + C≡C.²⁵ This suggested that the formation of HKrCC is energetically unfavorable and that the C≡C species, which is lower in energy, is more likely to be detected by infrared analysis. Additional experiments have included the synthesis of diacetylene xenon and krypton systems, HXeC₄H and HKrC₄H, respectively,²⁶ as well as the insertion of noble gas atoms (Ar, Kr, and Xe) into cyanoacetylene.²⁷ Both of these studies characterized the bonding through infrared spectroscopy and also included MP2 computations with a triple- ζ quality (6-311++G(2d,2p)) basis set on H, Kr, and C and an 18 electron relativistic effective core potential on Xe (LJ18).

Other recent theoretical studies have examined the bonding of noble gases to silicon.^{28–30} These studies have suggested that FXeSiF, FXeSiF₃, HXeSiF₃, and FArSiF₃ are chemically bound molecules.^{28,29} Our recent work has suggested that FKrSiF₃ is chemically bound and furthermore was the first study that showed that krypton is capable of forming chemical bonds to germanium.³⁰

This work investigates a number of potential new noble gas-bonded compounds, XNgCCNgX and XNgCCX (Ng = Kr, Ar; X = F, Cl, Br), which stem from the analogous HXeCCXeH and HXeCCH molecules. It is proposed that the fluorinated systems should be more stable than the krypton–hydride species, HKrCCKrH and HKrCC,²⁵ and that a dikrypton species

[†] Part of the “Thom H. Dunning, Jr., Festschrift”.

* Corresponding author. Fax: +1 940 565 418. E-mail: akwilson@unt.edu.

TABLE 1: FKrCCKrF and FCCKrF Optimal Geometries^a

method	Basis	FKrCCKrF			FKrCCF			
		F–Kr	Kr–C	C–C	F–Kr	Kr–C	C–C	C–F
B3LYP	cc-pVnZ							
	n = D				1.973	1.989	1.210	1.283
	n = T	1.961	1.965	1.205	1.967	1.952	1.196	1.274
	n = Q	1.966	1.955	1.203	1.974	1.941	1.194	1.273
	aug-cc-pVnZ							
	n = D	1.987	1.967	1.218	1.996	1.950	1.207	1.281
	n = T	1.976	1.952	1.204	1.986	1.937	1.194	1.274
	n = Q	1.973	1.950	1.203	1.983	1.936	1.194	1.272
	MP2	cc-pVnZ						
n = D					1.961	1.986	1.229	1.288
n = T		1.933	1.949	1.226	1.936	1.934	1.211	1.277
n = Q		1.937	1.933	1.222	1.942	1.918	1.207	1.274
aug-cc-pVnZ								
n = D		1.977	1.967	1.244	1.982	1.945	1.228	1.292
n = T		1.954	1.934	1.225	1.961	1.917	1.210	1.276
n = Q		1.947	1.929	1.222	1.955	1.913	1.207	1.273
CCSD(T)		aug-cc-pVnZ						
	n = D	1.987	1.986	1.237	1.993	1.965	1.225	1.296
	n = T	1.963	1.948	1.218	1.971	1.931	1.206	1.278

^a Bond lengths in Å.

(FKrCCKrF) may be stable enough to be detected through infrared analysis. Also, our work suggests that FArCCF could provide a stable enough structure to be synthesized experimentally, possibly becoming the second known chemically bonded argon molecule. Another similar molecule, FArCCH, has already been studied theoretically, and thus, this study adds to the list of possible organo-argon compounds.^{28,29}

II. Methodology

Optimal geometries, vibrational frequencies, charge distributions, and relative energies of the ground-state molecules were computed. These computations were performed using the B3LYP^{31,32} hybrid density functional and the ab initio methods, MP2³³ and CCSD(T).^{34–36} These methods were used in combination with the correlation consistent basis sets (cc-pVnZ) developed by Dunning et al.^{37–39} Previously, benchmark studies have shown that coupling the correlation consistent basis sets with CCSD(T) can provide accurate (~ 1 – 2 kcal/mol) energetics (i.e., atomization energies, ionization energies, electron affinities, ...) for fluorine–krypton bonded systems.⁴⁰ For noble gas systems that contain fluorine–krypton bonding, B3LYP, MP2, and CCSD(T) have provided qualitatively similar structural and energetic properties.³⁰ However, the validity of using DFT for the accurate prediction of noble gas bonded systems has been questioned in the past because it has falsely predicted a few HNgX systems to be metastable;¹⁰ therefore, MP2 and CCSD(T) were also used in this study.

Due to the computational cost, aug-cc-pVQZ was the largest basis set used for geometry optimizations and vibrational frequency calculations with MP2, and aug-cc-pVTZ was the largest basis set used in the CCSD(T) calculations. Charge distributions were calculated using the natural bond order (NBO) analysis at the B3LYP/aug-cc-pVTZ level of theory, enabling a qualitative description of the charge separation in the noble gas bonds. Our previous studies demonstrated that relative charge distributions vary little with respect to choice of correlated method;^{30,41} thus, only B3LYP was used in this study.

Relative energies have been useful in previous noble gas studies to provide an energy ordering of the various metastable species with respect to the energy of the noble gas and precursor molecule.^{12,14,19,21,25,30,41} For example, the previous study¹⁹ on HXeCC and HXeCCXeH demonstrates the significance of rela-

tive energy computations by predicting the stability of HXeCC and HXeCCXeH prior to experimental observation. These species were found later during characterization of HXeCCH.^{20,21} Due to the utility of relative energies, they were examined in this study, in which the energies of the noble gas compounds were computed relative to Ng + XCCX, which is the sum of the energies of the unbound noble gas (Ng) and the precursor molecule (XCCX). Also, several combinations of the constituent atoms of the XNgCCNgX compounds were considered. All of these relative energies were determined using B3LYP and MP2 computations paired with the aug-cc-pVQZ basis set and also using CCSD(T) paired with the aug-cc-pVTZ basis set.

Transition-state structures were identified for both the XNgCCNgX and XNgCCX molecules using the quadratic steepest descent (QSD) method,^{42,43} and energy and frequency calculations for transition-state structures were performed using MP2 at the aug-cc-pVDZ, aug-cc-pVTZ, and aug-cc-pVQZ basis set levels. Intrinsic reaction coordinate (IRC) calculations also were performed at these levels of theory to verify the transition structure as the barrier in the decomposition pathway.

Density functional computations were performed using the GAUSSIAN 03 software suite,⁴⁴ and the MP2 and CCSD(T) computations were performed using the MOLPRO quantum chemistry package.⁴⁵

III. Results and Discussion

A. Minimum Energy Structures. Optimal geometries, as shown in Table 1, were found for the ground-state structures for FKrCCKrF and FKrCCF, in which both structures were found to be linear. It must be noted that, in Table 1, a number of double- ζ optimized geometries were excluded because the frequency analysis provided imaginary normal modes, which indicated that the structures found were not minimum energy structures. This was not surprising, as a double- ζ basis set did not correctly predict KrF₂ and HKrCl to be stable with respect to dissociation.^{40,41} However, both KrF₂ and HKrCl have been shown by experiment to exist^{3,46,47} and have been shown by computation to be stable when more flexible basis sets (at least aug-cc-pVTZ quality) were used. These previous studies^{40,41} suggest that smaller basis sets such as cc-pVDZ are inadequate for the description of krypton-bonded systems.

TABLE 2: ClKrCCKrCl and ClKrCCCl Optimal Geometries^a

method	basis set	ClKrCCKrCl			ClKrCCCl			
		Cl–Kr	Kr–C	C–C	Cl–Kr	Kr–C	C–C	C–Cl
B3LYP	cc-pVnZ							
	n = T	2.443	2.048	1.210	2.450	2.015	1.203	1.641
	n = Q	2.443	2.041	1.208	2.452	2.007	1.202	1.637
	aug-cc-pVnZ							
MP2	n = T	2.446	2.042	1.209	2.456	2.009	1.203	1.640
	n = Q	2.444	2.041	1.208	2.454	2.005	1.202	1.637
	cc-pVnZ							
	n = T				2.394	2.023	1.224	1.636
	n = Q	2.392	2.043	1.232	2.390	2.004	1.220	1.631
	aug-cc-pVnZ							
	n = T				2.402	2.012	1.224	1.635
	n = Q	2.395	2.043	1.233	2.393	2.003	1.220	1.630
CCSD(T)	aug-cc-pVnZ							
	n = D	2.514	2.145	1.247	2.499	2.090	1.234	1.668
	n = T	2.435	2.064	1.225	2.438	2.027	1.216	1.647

^a Bond lengths in Å.

Using large, flexible basis sets generally provided shorter bond lengths than smaller basis sets for FKrCCKrF and FKrCCF. Most of the krypton bond lengths reached convergence at the quadruple- ζ level and only change ~ 0.005 Å from the triple- ζ level to the quadruple- ζ level, when either B3LYP or MP2 was used. However, the F–Kr bond in FKrCCF did not converge monotonically with respect to increasing basis set size when B3LYP was used with the cc-pVnZ basis sets, such that the bond length changed from 1.973 to 1.967 and then to 1.974 at $n = D, T,$ and $Q,$ respectively. This non-monotonic convergence was resolved when diffuse functions were used, as shown by the B3LYP/aug-cc-pVnZ results in Table 1. [The unusual non-monotonic convergence of molecular properties with respect to increasing size of the correlation consistent basis sets has been observed for several density functionals by Wang and Wilson.^{48–50} They have shown that diffuse functions, as well as other factors, can help improve the convergence behavior of properties for some molecules.] The inclusion of diffuse functions in the basis sets generally provided longer F–Kr bond lengths and shorter Kr–C bond lengths than were found using the standard correlation consistent basis sets. Upon the second insertion of krypton into the acetylene derivative, there was a slight shortening (~ 0.008 Å) in the F–Kr bond, while a lengthening occurred for the Kr–C and C–C bonds by 0.015 and 0.012 Å, respectively. In a previous study on HXeCCXeH, a slight change in geometry was also reported, in which the H–Xe and C–C bonds were lengthened by 0.027 and 0.016 Å, respectively, while the Xe–C bond decreased by 0.008 Å.¹⁹ In both the current study and the HXeCCXeH study,¹⁹ the bond distance from the noble gas atom to the most electronegative atom decreased upon the addition of the second noble gas atom.

The computed krypton–carbon bond lengths in FKrCCKrF and FKrCCF are slightly shorter than those predicted in previous computational studies of krypton–carbon-bonded molecules. For example, the current MP2/aug-cc-pVQZ calculations predicted a Kr–C bond length of 1.913 Å in FKrCCF, whereas our previous work predicted a Kr–C bond length of 2.061 Å in FKrCF₃ using MP2/aug-cc-pVQZ.³⁰ Also, Khriachtchev et al. reported a Kr–C bond length of 2.25 Å in HKrCCH from their MP2(full)/aug-cc-pVDZ computation.²⁵ Their Kr–C bond length was much longer (0.28 Å) than the Kr–C length in FKrCCF, shown in Table 1. Likewise, the F–Kr bond length in FKrCCKrF, as computed at the MP2/aug-cc-pVTZ level (1.954 Å), was significantly shorter than the bond length found in HKrF (2.034 Å), which was computed by Chaban and co-workers⁶ at the same level of theory. With knowledge that a shorter bond

length generally corresponds to a stronger bond, both the single and double insertion of krypton into FCCF should provide a more stable noble gas bonded system in comparison to the analogous systems, HKrCCH and HKrCCKrH.

In addition to the fluorine analogues, ClKrCCKrCl and ClKrCCCl were also found to be stable, ground-state structures, and the optimal geometries are listed in Table 2. As noted in Table 1, ground-state structures could not be determined at lower basis set levels for the chlorine–krypton molecules in Table 2. In fact, MP2 required a quadruple- ζ level basis set to provide stable, ground-state structures for ClKrCCKrCl. As shown in Table 1, upon the second insertion of Kr into the precursor (FCCF), the F–Kr bond length contracts; however, as shown in Table 2, the Cl–Kr bond length does not contract when MP2 and CCSD(T) were used. The other bonds (Kr–C and C–C) in the chlorine–krypton molecule are generally lengthened upon the second krypton insertion, which is similar to the fluorine–krypton system. In comparison to previous computational studies of Cl–Kr-bonded molecules, the Cl–Kr bonding in both of the new systems was much shorter (~ 0.1 Å). For example, in HKrCl the Kr–Cl bond was 2.529 Å at the CCSD(T)/aug-cc-pVTZ level,⁴¹ whereas the Cl–Kr bond lengths were 2.435 and 2.438 Å for ClKrCCKrCl and ClKrCCCl, respectively, as shown in Table 2. There are difficulties in predicting ground-state structures for ClKrCCKrCl, which are discussed further in the Relative Energy section.

Fluorine–argon analogues were also predicted to be stable, ground-state structures, and their bond lengths are given in Table 3. Again, double- ζ basis sets were not flexible enough to predict stable, ground-state structures for these noble gas systems. Overall, the bonding trends for the fluorine–argon systems are very similar to those found for fluorine–krypton (Table 1), with a contraction (~ 0.008 Å) of the halogen–noble gas bond (the F–Ar bond), upon the insertion of the second noble gas (argon). Also, the F–Ar bonding in FArCCArF and FArCCF is nearly 0.1 Å shorter than that in HArF, which was shown by Chaban et al. to be 1.983 Å with MP2/aug-cc-pVTZ and 1.993 Å by Runeberg et al. with CCSD(T)/aug-cc-pVTZ.¹²

Overall, each of these six molecules are stable, ground-state structures which surprisingly provide shorter X–Ng bond distances than the similar smaller HNgX species that have been characterized in earlier studies.^{6,12,41}

Note that the exclusion of ClArCCArCl and ClArCCCl, the logical complements to the class of compounds investigated in this study, is intentional. Among the geometry optimizations that converged to bound structures of ClArCCArCl and

TABLE 3: FArCCArF and FArCCF Optimal Geometries^a

method	basis set	FArCCArF			FArCCF			
		F–Ar	Ar–C	C–C	F–Ar	Ar–C	C–C	C–F
B3LYP	cc-pVnZ							
	n = T	1.899	1.860	1.203	1.908	1.836	1.193	1.272
	n = Q	1.899	1.834	1.200	1.912	1.812	1.191	1.271
	aug-cc-pVnZ							
MP2	n = T	1.914	1.839	1.201	1.931	1.813	1.192	1.272
	n = Q	1.906	1.828	1.200	1.923	1.803	1.191	1.270
	cc-pVnZ							
	n = T				1.859	1.849	1.211	1.276
CCSD(T)	n = Q	1.861	1.845	1.222	1.864	1.804	1.206	1.272
	aug-cc-pVnZ							
	n = T	1.882	1.863	1.227	1.887	1.809	1.209	1.275
	n = Q	1.870	1.834	1.221	1.879	1.790	1.205	1.272
CCSD(T)	aug-cc-pVnZ							
	n = T	1.912	1.878	1.217	1.917	1.834	1.204	1.277

^a Bond lengths in Å.**TABLE 4: Natural Bond Order Charge Distributions (B3LYP/aug-cc-pVTZ)**

Atoms	XNgCCNgX			XNgCCX				
	X	Ng	C	X	Ng	C	C	X
X = F, Ng = Kr	-0.6130	0.7443	-0.1313	-0.6269	0.6732	0.1200	0.0031	-0.1693
X = Cl, Ng = Kr	-0.4792	0.5893	-0.1101	-0.5146	0.5962	-0.0033	-0.0451	-0.0331
X = F, Ng = Ar	-0.5761	0.5313	0.0448	-0.5861	0.5056	0.1746	0.1068	-0.2008

ClArCCl, two imaginary frequencies were identified during the vibrational frequency analysis of each molecule using every combination of B3LYP and MP2 methods with cc-pVnZ and aug-cc-pVnZ basis sets, where $n = D, T,$ and Q . Two other logical candidates for halogen-containing organo-noble gas compounds related to those studied here are BrKrCCrBr and BrArCCArBr. While B3LYP used in conjunction with the cc-pVnZ and aug-cc-pVnZ basis sets (where $n = D, T, Q$) predicts two imaginary frequencies in the vibrational spectrum of BrArCCArBr, MP2 optimizations do not converge with cc-pVnZ or aug-cc-pVnZ, where $n = D, T,$ and Q . Interestingly, B3LYP predicts ground-state structures for BrKrCCrBr with basis sets cc-pVnZ and aug-cc-pVnZ, where $n = T$ and Q , but MP2 does not. This is possibly a case where density functional theory is falsely predicting ground-state structures, as has been noted in past computational studies of noble-gas-bonded compounds such as HHeI, HNeCl, HNeBr, and HNeI.¹⁰

B. Charge Distribution. For each molecule, charge distribution calculations indicate highly positive charges on the krypton/argon atoms, highly negative charges on the halogens, and relatively neutral charges on the carbon atoms. These computed partial charges are shown in Table 4. A large charge separation generally aids in the stability of these molecules and is characteristic of the resonance between the somewhat ionic and covalent nature of noble gas bonding.⁵¹ In a similar system, HKrCCH,²⁵ the charge on Kr was 0.535, which is slightly less than the charge on Kr in the FKrCCF and ClKrCCCl systems. In comparison to the HKrCCH systems, there is an obvious difference in the charge on the carbons and is due to the highly electronegative carbons in CCH, which causes the charge to be much larger (~ -0.4) on the carbons, while, in CCF and CCCL, the halogen is the electronegative species and carries the largest charge (~ -0.6). The highly ionic character of the F–Kr bond in the dikrypton system, with a charge separation of 1.3573 between F and Kr, suggests that FKrCCrF should be fairly stable. A smaller ionic character was found in the Cl–Kr and F–Ar bonds (i.e., a smaller charge separation) in comparison to that from F–Kr, which indicates that ClKrCCrCl and FArCCArF should not be as stable as FKrCCrF.

TABLE 5: Relative Energies in eV

species	method (basis set)		
	B3LYP (aug-cc-pVQZ)	MP2 (aug-cc-pVQZ)	CCSD(T) (aug-cc-pVTZ)
C ₂ F ₂ + 2Kr	0.000	0.000	0.000
FKrCCF + Kr	4.028	3.945	4.097
FCC + 2Kr + F	5.511	6.123	5.464
FKrCCrF	8.275	8.070	8.386
F ₂ + C ₂ + 2Kr	9.846	8.952	8.487
KrF ₂ + C ₂ + Kr	10.204	9.210	9.149
FKrCC + Kr + F	<i>a</i>	10.005	9.665
2F + C ₂ + 2Kr	11.458	10.828	10.068
F ₂ + 2C + 2Kr	15.045	15.693	17.398
2F + 2C + 2Kr	16.657	17.569	18.979
2F ⁻ + 2C ⁺ + 2Kr	32.685	32.711	31.864
2F ⁻ + C ₂ ²⁺ + 2Kr	39.697	39.551	38.364
C ₂ Cl ₂ + 2Kr	0.000	0.000	0.000
ClKrCCCl + Kr	4.112	4.181	4.218
ClCC + 2Kr + Cl	4.625	5.409	4.712
Cl ₂ + C ₂ + 2Kr	7.254	6.514	6.109
ClKrCCrCl	8.241	8.345	8.434
2Cl + C ₂ + 2Kr	9.632	9.174	8.399
Cl ₂ + 2C + 2Kr	12.454	13.255	15.020
2Cl + 2C + 2Kr	14.832	15.915	17.310
2Cl ⁻ + 2C ⁺ + 2Kr	30.565	31.040	29.842
2Cl ⁻ + C ₂ ²⁺ + 2Kr	37.577	37.880	36.342
C ₂ F ₂ + 2Ar	0.000	0.000	0.000
FArCCF + Ar	5.103	5.173	5.324
FCC + 2Ar + F	5.511	6.123	5.464
F ₂ + C ₂ + 2Ar	9.846	8.952	8.487
FArCCArF	10.448	10.513	10.828
2F + C ₂ + 2Ar	11.458	10.828	10.068
F ₂ + 2C + 2Ar	15.045	15.693	17.398
2F + 2C + 2Ar	16.657	17.569	18.979
2F ⁻ + 2C ⁺ + 2Ar	32.685	32.711	31.864
2F ⁻ + C ₂ ²⁺ + 2Ar	39.697	39.551	38.364

^a B3LYP/aug-cc-pVQZ does not find FKrCC as a minimum.

C. Relative Energy. Relative energy calculations have been used in this study to provide an energy ordering of the various metastable species with respect to (or relative to) the energy of the noble gas and precursor molecule. In Table 5, the computed relative energies are shown for the six molecules, as well as for other molecular species that might occur during the formation/decomposition process. In this study, the FKrCCF

TABLE 6: Selected Fundamental Vibrational Frequencies (cm⁻¹) Computed with B3LYP and MP2 Together with the aug-cc-pVnZ Basis Set^a

molecule	$\nu_{stretch}$	B3LYP		MP2	
		n = T	n = Q	n = T	n = Q
FKrCCKrF	Kr-C(sym)	173 (0)	174 (0)	174 (0)	177 (0)
	F-Kr(asym)	461 (580)	463 (591)	503 (538)	509 (554)
	F-Kr(sym)	489 (0)	490 (0)	526 (0)	532 (0)
	Kr-C(asym)	553 (417)	555 (407)	564 (620)	574 (589)
	C-C(sym)	2215 (0)	2214 (0)	2081 (0)	2091 (0)
ClKrCCKrCl	Kr-C(sym)	131 (0)	131 (0)	<i>b</i>	120 (0)
	Cl-Kr(asym)	275 (341)	275 (349)		319 (16)
	Cl-Kr(sym)	304 (0)	303 (0)		343 (0)
	Kr-C(asym)	432 (920)	432 (922)		450 (1075)
	C-C(sym)	2161 (0)	2159 (0)		1990 (0)
FArCCArF	Ar-C(sym)	205 (0)	208 (0)	164 (0)	177 (0)
	F-Ar(asym)	458 (164)	464 (176)	407 (561)	443 (474)
	F-Ar(sym)	529 (0)	535 (0)	592 (0)	596 (0)
	Ar-C(asym)	550 (1146)	557 (1140)	588 (1258)	582 (1381)
	C-C(sym)	2224 (0)	2225 (0)	2044 (0)	2071 (0)
FKrCCF	Kr-C	326 (40)	326 (40)	330 (62)	335 (58)
	F-Kr	471 (274)	473 (275)	508 (296)	513 (299)
	C-C	2386 (285)	2381 (285)	2305 (285)	2309 (283)
ClKrCCCl	Kr-C	223 (31)	224 (31)	208 (82)	213 (77)
	Cl-Kr	294 (235)	293 (237)	337 (195)	337 (202)
	C-C	2244 (222)	2241 (223)	2120 (221)	2128 (221)
FArCCF	Ar-C	329 (19)	332 (18)	298 (129)	315 (106)
	F-Ar	506 (497)	512 (411)	555 (471)	557 (485)
	C-C	2401 (313)	2397 (313)	2309 (345)	2318 (341)

^a Vibrational intensities are listed in parentheses (km/mol). ^b ClKrCCKrCl is not a minimum at the MP2/aug-cc-pVTZ level.

molecule was the lowest in energy relative to the most stable combination of the constituent atoms, C₂F₂ + 2Kr. As shown in Table 5, the relative energy of the second krypton insertion is roughly twice that of the first insertion.

The relative energy ordering of each of the molecular species in Table 5 was found to be the same with each computational method used. The most noticeable difference in the MP2 and CCSD(T) relative energies was the energy change between FKrCCKrF and F₂ + C₂ + 2Kr; for MP2 this difference was 0.882 eV, and for CCSD(T) it was 0.101 eV. It would appear that the more sophisticated CCSD(T) level of theory (which should recover more correlation energy) predicted the FKrCCKrF system to be less stable and closer to the energy of the F₂ + C₂ + 2Kr system. However, this result was contrary to the idea that krypton-bonded systems rely heavily on electron correlation to be bound, which has been shown previously for KrF₂ and HKrCl.^{40,41} Further inspection of this result revealed that the correlation energy in FKrCCKrF described by the MP2/aug-cc-pVQZ (-1.372 697 E_h) computation was larger than that of the CCSD(T)/aug-cc-pVTZ (-1.352 754 E_h) computation, which showed the large dependence on basis set size for energetic properties of noble gas-bonded systems. It must be noted, however, that two recent studies have shown how MP2 can be an inadequate level of theory at predicting the stability of HNgY molecules. For example, HArC₆H was predicted to be 1.14 eV more stable than H + Ar + C₆H whereas B3LYP predicted this molecule to be unstable (-0.65 eV).^{52,53} Lignell et al. attributed this deviation to the larger error (2.16 eV) they found in computing the dissociation energy of H₂C₆ with MP2 in comparison to B3LYP with an error only of 0.12 eV. However, in the current study the CCSD(T) relative energies provide the same energetic ordering for each of the systems studied as MP2.

In the experimental synthesis of HXeCCH, two other xenon systems were also detected by infrared spectroscopy, HXeC-CXeH and HXeCC.²¹ However, as mentioned previously, the HKrCCH experimental study did not detect either HKrCCKrH or HKrCC.²⁵ From the relative energy predictions in Table 5,

upon formation of FKrCCF, finding FKrCCKrF by infrared spectroscopy might be possible, since FKrCCKrF was found to be lower in energy compared to nearly all of its dissociated parts. The detection of FKrCC is, however, not as likely because FKrCC has a much higher relative energy, 1.935 eV above the MP2-computed FKrCCKrF structure.

The relative energies of both the chlorine-krypton and fluorine-argon species were qualitatively different from the relative energies of the fluorine-krypton systems. For example ClKrCCKrCl was less stable than Cl₂ + C₂ + 2Kr by 1.891 eV, and likewise for FArCCArF, which was 2.341 eV less stable than F₂ + C₂ + 2Ar. Because ClKrCCKrCl and FArCCArF were both energetically unfavorable, neither of these two species is likely to form a ground-state structure that is detectable by infrared spectroscopy. It must also be noted that the ClKrCC and FArCC were not included in the relative energy tables, since no minimum energy ground-state structures could be found, even at the MP2/aug-cc-pVQZ level. Furthermore, KrCl₂ and ArF₂ were not included since experimentalists have previously provided evidence that these molecules do not exist.⁵⁴ The relative energies of the chlorine-krypton and fluorine-argon species did not always provide the same qualitative ordering from one method to another as compared to the fluorine-krypton species. The CCSD(T)-calculated relative energy values for ClKrCCKrCl (8.434 eV) and FArCCArF (10.828 eV) were actually higher in energy than the species 2Cl + C₂ + 2Kr and 2F + C₂ + 2Ar, respectively, which further demonstrated the instability of the chlorine-krypton and fluorine-argon species.

D. Vibrational Frequencies. In past noble gas-bonding studies, vibrational frequencies have been the sole analysis, which has allowed experimentalists to compare directly to theoretically determined data. For the six compounds found in this study, the fundamental stretching frequencies that involve a noble gas atom have been selected and are listed in Table 6. In addition, the C≡C stretching frequencies in each of these molecules have also been included. The basis set dependence for the normal modes listed in Table 6 was small when either B3LYP or MP2 was used. In fact, there were only two instances

TABLE 7: Transition-State Structure for XNgCCNgX (MP2/aug-cc-pVnZ)

molecule	basis set aug-cc-pVnZ	bond length (Å)					bond angle (deg)			
		X–Ng	Ng–C	C–C	C–Ng	Ng–X	XNgC	NgCC	CCNg	CNgX
FKrCCKrF	n = T	2.300	1.772	1.218	1.952	1.929	98.1	174.6	179.2	180.0
	n = Q	2.291	1.769	1.214	1.946	1.922	98.2	174.7	179.2	180.0
ClKrCCKrCl	n = Q	2.838	1.780	1.220	2.076	2.359	98.2	172.7	169.1	178.8
FArCCArF	n = T	2.236	1.630	1.215	1.905	1.857	101.4	175.6	175.1	179.6
	n = Q	2.221	1.623	1.211	1.872	1.843	101.4	174.3	178.1	179.8

TABLE 8: Transition-State Structures for XNgCCX (MP2/aug-cc-pVnZ)

molecule	basis set aug-cc-pVnZ	bond length (Å)				bond angle (deg)		
		X–C	C–C	C–Ng	Ng–X	XCC	CCNg	CNgX
FCCKrF	n = T	1.264	1.203	1.769	2.318	175.0	166.8	98.0
	n = Q	1.262	1.198	1.766	2.307	179.9	172.9	98.3
ClCCrCl	n = T	1.615	1.221	1.782	2.859	171.6	152.3	97.9
	n = Q	1.613	1.211	1.772	2.844	179.9	163.7	97.5
FCCArF	n = T	1.259	1.208	1.634	2.256	169.3	154.2	101.7
	n = Q	1.257	1.204	1.627	2.244	170.1	155.7	101.6

when the frequencies varied by more than 20 cm⁻¹ from aug-cc-pVTZ to aug-cc-pVQZ, which with MP2 were the F–Ar(asym) and C–C(asym) stretches in FArCCArF. For the molecules containing krypton, the frequencies involving a krypton stretch were generally larger when computed with MP2 than with B3LYP. The C–C stretch in all of the noble gas molecules in this study was generally 100 cm⁻¹ smaller when computed with MP2 instead of B3LYP. Therefore, it appears that the electron density for the C≡C bond is less for MP2 than it is for B3LYP and is more for the Kr–C bond with MP2 than it is for B3LYP. In the three centrosymmetric molecules (FKrCCKrF, ClKrCCKrCl, FArCCArF), both the symmetric and antisymmetric vibrational modes were included in Table 6. To aid in future experimental identification of these molecules, the vibrational intensities have also been included in Table 6. It must be noted that only the antisymmetric vibrational modes are infrared active in these three molecules, thus having a nonzero intensity. In comparison to the intensity of the C–C stretch in FKrCCF, ClKrCCCl, and FArCCF, the intensity of the noble gas halide (Ng–X) stretch is of similar magnitude, and therefore, upon the formation of the Ng–X bond, detection of this vibrational mode should be feasible.

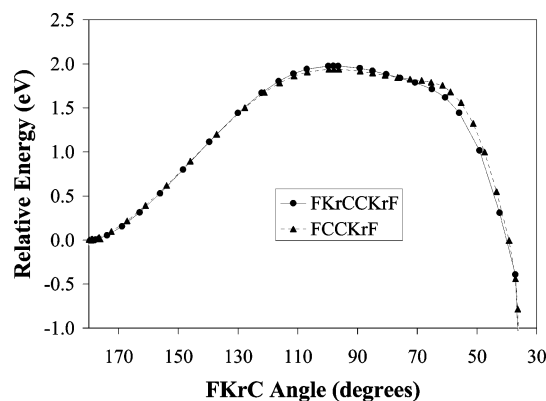
E. Transition States. The transition-state structures corresponding to the removal of each noble gas atom from the XNgCCNgX molecules are shown in Tables 7 and 8. In FKrCCKrF, the favorable decomposition pathway for the removal of the first noble gas atom should involve a bending of the F–Kr–C bond angle, since other dissociations would lead to unfavorable higher energy products. For FKrCCKrF, a transition state was located with an F–Kr–C angle at 98.2°, which was coupled with an increase in F–Kr bond length and a departure from linearity among the atoms in the distal CCKrF chain. The removal of the second krypton atom had a reaction barrier and pathway similar to that for the removal of the first krypton, and a transition state was found at a 98.0° F–Kr–C angle. The MP2/aug-cc-pVnZ-computed dissociation barriers are listed in Table 9. Using MP2 to compute the dissociation barriers of these noble gas systems is not thought to produce much deviation from CCSD(T) results as compared with computing the enthalpy of reaction, in which 10–15 kcal/mol separated the MP2 and CCSD(T) energies, as shown by Li et al.⁵³ Interestingly, the energy barrier for the removal of the first krypton was larger (~0.045 eV) than the energy barrier for the removal of the second krypton. The dissociation barrier in FKrCCF was only slightly lower than the barrier predicted for

TABLE 9: Decomposition Barriers in eV (MP2/aug-cc-pVnZ)

molecule	basis set aug-cc-pVnZ	barrier
FKrCCKrF	n = T	1.987
	n = Q	1.999
FKrCCF	n = T	1.942
	n = Q	1.958
ClKrCCKrCl	n = T	1.777
	n = Q	1.681
ClKrCCCl	n = T	1.681
	n = Q	1.690
FArCCArF	n = T	1.636
	n = Q	1.647
FArCCF	n = T	1.504
	n = Q	1.520

HXeCCH (2.18 eV) by Lundell et al.¹⁹ Intrinsic reaction coordinate analyses verified these structures as the transition structures to the dissociated products and are shown in Figure 1. The reaction pathways shown are plotted with respect to the F–Kr–C angle, as this angle is the principle geometric parameter that was changed from the ground state to the transition state. The bending of the F–Kr–C angle also lies on the transition vector determined from the imaginary mode of the vibrational frequencies. This figure is very similar to the one presented in the Lundell et al. study on HXeCCH because they both provide fairly high (~2.0 eV) and wide energy barriers.¹⁹

Both ClKrCCKrCl and FArCCArF were found to have a similar transition state to FKrCCKrF with a bending of the X–Ng–C angle and an elongation of the X–Ng bond although

**Figure 1.** Minimum energy dissociation of FKrCCKrF and FCCKrF through the F–Kr–C bending angle (MP2/aug-cc-pVTZ).

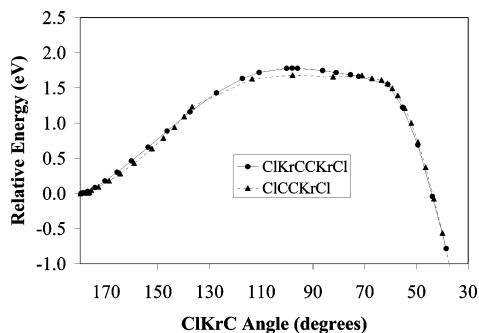


Figure 2. Minimum energy dissociation of ClKrCCKrCl and ClCCKrCl through the Cl–Kr–C bending angle (MP2/aug-cc-pVQZ).

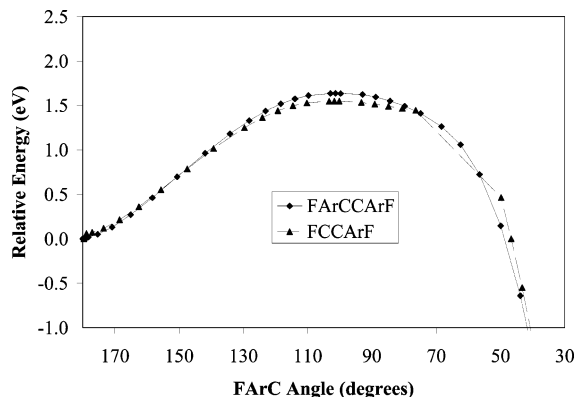


Figure 3. Minimum energy dissociation of FArCCArF and FCCArF through the F–Ar–C bending angle (MP2/aug-cc-pVTZ).

as suggested by the relative energy comparison, other dissociation channels might be energetically favorable for ClKrCCKrCl and FArCCArF, since both of these molecules were higher in energy and could dissociate to $\text{Cl}_2 + \text{C}_2 + 2\text{Kr}$ and $\text{F}_2 + \text{C}_2 + 2\text{Ar}$, respectively. However, in this study only the transition through the bending angle was chosen to make a simple comparison with the FKrCCKrF dissociation. The computed dissociation barriers of ClKrCCKrCl (1.777 eV) and FArCCArF (1.647 eV) were found to be significantly smaller than the barrier of FKrCCKrF, further illustrating their decreased stability in comparison to FKrCCKrF (shown earlier in the Relative Energies section). In the fluorine–krypton system, the barrier to remove the first noble gas atom was slightly larger (~ 0.1 eV) than for the removal of the second noble gas atom. The intrinsic reaction coordinate computations are shown in Figures 2 and 3 for the chlorine–krypton and fluorine–argon systems, respectively. For both of these systems, there was a broad transition barrier through the bending of the X–Ng–C angle as was observed for the fluorine–krypton species.

IV. Conclusions

Four new organo-krypton compounds (FKrCCF, FKrCCKrF, ClKrCCKrCl, ClKrCCCl) have been successfully identified and characterized theoretically as well as two new organo-argon molecules (FArCCArF and FArCCF). The optimized geometries suggest that these molecules have some of the shortest noble gas bonds known, and vibrational frequency calculations verify them as ground-state structures. FKrCCKrF is the first known metastable centrosymmetric organokrypton molecule and is similar to the HXeCCXeH reported previously.²¹ In each of the six molecules, the charge distribution indicates highly positive charges on the noble gas atoms, highly negative charges on the halogen atoms, and relatively neutral charges on the carbon atoms. Relative energy calculations predict the FKrCCF mol-

ecules to be the lowest in energy relative to the precursor, $\text{C}_2\text{F}_2 + 2\text{Kr}$, and predict FKrCCKrF to be the next most stable structure. Also, ClKrCCCl and FArCCCl were found to be the lowest in energy relative to their precursors, $\text{C}_2\text{Cl}_2 + 2\text{Kr}$ and $\text{C}_2\text{F}_2 + 2\text{Ar}$, respectively, but ClKrCCKrCl and FArCCArF were not the most stable structures computed. The XNgCCNgX and XNgCCX transition structures were found with a large bent X–Ng–C angle, which should be the major channel in the decomposition. This study predicts that, upon the formation of FKrCCF, the first experimentally detectable dikrypton system (FKrCCKrF) should be observed. However, upon the formation of FArCCF or ClKrCCCl, it is thought that only trace amounts of FArCCArF and ClKrCCKrCl might be formed due to their unfavorable energetic stability and that they might be undetectable with infrared spectroscopy matrix isolation techniques.

Acknowledgment. We gratefully acknowledge support from a National Science Foundation CAREER Award (Grant CHE-0239555) and the University of North Texas Faculty Research Grant Program. Computational resources were provided via the National Science Foundation (Grant CHE-0342824) and by the National Computational Science Alliance; this latter support was for access to their NCSA IBM p690 under No. CHE010021. Additional support was provided by the University of North Texas Academic Computing Services for the use of the UNT Research Cluster. The Center for Advanced Scientific Computing and Modeling has been supported by a grant from the U.S. Department of Education.

References and Notes

- (1) Pauling, L. *J. Am. Chem. Soc.* **1933**, *55*, 1895.
- (2) Bartlett, N. *Proc. Chem. Soc.* **1962**.
- (3) Pettersson, M.; Lundell, J.; Rasanen, M. *J. Chem. Phys.* **1995**, *102*, 6423.
- (4) Jolkkonen, S.; Pettersson, M.; Lundell, J. *J. Chem. Phys.* **2003**, *119*, 7356.
- (5) Lundell, J.; Khriachtchev, L.; Pettersson, M.; Rasanen, M. *Low Temp. Phys.* **2000**, *26*, 680.
- (6) Chaban, G. M.; Lundell, J.; Gerber, R. B. *Chem. Phys. Lett.* **2002**, *364*, 628.
- (7) Johansson, M.; Hotokka, M.; Pettersson, M.; Rasanen, M. *Chem. Phys.* **1999**, *244*, 25.
- (8) Khriachtchev, L.; Pettersson, M.; Runeberg, N.; Lundell, J.; Rasanen, M. *Nature* **2000**, 406.
- (9) Lundell, J.; Chaban, G. M.; Gerber, R. B. *Chem. Phys. Lett.* **2000**, *331*, 308.
- (10) Panek, J.; Latajka, Z.; Lundell, J. *Phys. Chem. Chem. Phys.* **2002**, *4*, 2504.
- (11) Pettersson, M.; Lundell, J.; Rasanen, M. *Eur. J. Inorg. Chem.* **1999**, *5*, 729.
- (12) Runeberg, N.; Pettersson, M.; Khriachtchev, L.; Lundell, J. *J. Chem. Phys.* **2001**, *114*, 836.
- (13) Takayanagi, T. *Chem. Phys. Lett.* **2003**, *371*, 675.
- (14) Wong, M. W. *J. Am. Chem. Soc.* **2000**, *122*, 6289.
- (15) Yen, S.-Y.; Mou, C.-H.; Hu, W.-P. *Chem. Phys. Lett.* **2004**, *383*, 606.
- (16) Yockel, S.; Seals, J. J. I.; Wilson, A. K. *Chem. Phys. Lett.* **2004**, *393*, 448.
- (17) Chaban, G. M. *Chem. Phys. Lett.* **2004**, *395*, 182.
- (18) McDowell, S. A. C. *Phys. Chem. Chem. Phys.* **2003**, 1530.
- (19) Lundell, J.; Cohen, A.; Gerber, R. B. *J. Phys. Chem. A* **2002**, *106*, 11950.
- (20) Feldman, V. I.; Sukhov, F. F.; Orlov, A. Y.; Tyulpina, I. V. *J. Am. Chem. Soc.* **2003**, *125*, 4698.
- (21) Khriachtchev, L.; Tanskanen, H.; Lundell, J.; Pettersson, M.; Kiljunen, H.; Rasanen, M. *J. Am. Chem. Soc.* **2003**, *125*, 4696.
- (22) Burger, H.; Schneider, W.; Sommer, S.; Thiel, W. *J. Chem. Phys.* **1991**, *95*, 5660.
- (23) McNaughton, D.; Elmes, P. *Spectrochim. Acta* **1992**, *48A*, 605.
- (24) Friedrich, H. B.; Tardy, D. C.; Burton, D. J. *J. Fluorine Chem.* **1993**, *65*, 53.
- (25) Khriachtchev, L.; Tanskanen, H.; Cohen, A.; Gerber, R. B.; Lundell, J.; Pettersson, M.; Kiljunen, H.; Rasanen, M. *J. Am. Chem. Soc.* **2003**, *125*, 6876.

- (26) Tanskanen, H.; Khriachtchev, L.; Lundell, J.; Kiljunen, H.; Rasanen, M. *J. Am. Chem. Soc.* **2003**, *125*, 16361.
- (27) Khriachtchev, L.; Lignell, A.; Tanskanen, H.; Lundell, J.; Kiljunen, H.; Rasanen, M. *J. Phys. Chem. A* **2006**, *110*, 11876.
- (28) Lundell, J.; Panek, J.; Latajka, Z. *Chem. Phys. Lett.* **2001**, *348*, 147.
- (29) Cohen, A.; Lundell, J.; Gerber, R. B. *J. Chem. Phys.* **2003**, *119*, 6415.
- (30) Yockel, S.; Garg, A.; Wilson, A. K. *Chem. Phys. Lett.* **2005**, *411*, 91.
- (31) Becke, A. D. *J. Chem. Phys.* **1993**, *98*, 5648.
- (32) Lee, C.; Yang, W.; Parr, R. G. *Phys. Rev.* **1988**, *B37*, 785.
- (33) Möller, C.; Plesset, M. S. *Phys. Rev. B* **1934**, *46*, 618.
- (34) Watts, J. D.; Gauss, J.; Bartlett, R. J. *J. Chem. Phys.* **1993**, *98*, 8718.
- (35) Purvis, G. D. I.; Bartlett, R. J. *J. Chem. Phys.* **1982**, *76*, 1910.
- (36) Raghavachari, K.; Trucks, G. W.; Pople, J. A.; Head-Gordon, M. *Chem. Phys. Lett.* **1989**, *157*, 1989.
- (37) Dunning, T. H., Jr. *J. Chem. Phys.* **1989**, *90*, 1007.
- (38) Woon, D. E.; Dunning, T. H., Jr. *J. Chem. Phys.* **1992**, *98*, 1358.
- (39) Wilson, A. K.; Woon, D. E.; Peterson, K. A.; Dunning, T. H., Jr. *J. Chem. Phys.* **1999**, *110*, 7667.
- (40) Yockel, S.; Mintz, B.; Wilson, A. K. *J. Chem. Phys.* **2004**, *121*, 60.
- (41) Yockel, S.; Seals, J. J., III; Wilson, A. K. *Chem. Phys. Lett.* **2004**, *393*, 448.
- (42) Sun, J.; Ruedenberg, K. *J. Chem. Phys.* **1993**, *99*, 5269.
- (43) Sun, J.; Ruedenberg, K. *J. Chem. Phys.* **1994**, *101*, 2157.
- (44) Frisch, M. J.; Trucks, G. W.; Schlegel, H. B.; Scuseria, G. E.; Robb, M. A.; Cheeseman, J. R.; Montgomery, J. A., Jr.; T. V.; Kudin, K. N.; Burant, J. C.; Millam, J. M.; Iyengar, S. S.; Tomasi, J.; Barone, V.; Mennucci, B.; Cossi, M.; Scalmani, G.; Rega, N.; Petersson, G. A.; Nakatsuji, H.; Hada, M.; Ehara, M.; Toyota, K.; Fukuda, R.; Hasegawa, J.; Ishida, M.; Nakajima, T.; Honda, Y.; Kitao, O.; Nakai, H.; Klene, M.; Li, X.; Knox, J. E.; Hratchian, H. P.; Cross, J. B.; Bakken, V.; Adamo, C.; Jaramillo, J.; Gomperts, R.; Stratmann, R. E.; Yazyev, O.; Austin, A. J.; Cammi, R.; Pomelli, C.; Ochterski, J. W.; Ayala, P. Y.; Morokuma, K.; Voth, G. A.; Salvador, P.; Dannenberg, J. J.; Zakrzewski, V. G.; Dapprich, S.; Daniels, A. D.; Strain, M. C.; Farkas, O.; Malick, D. K.; Rabuck, A. D.; Raghavachari, K.; Foresman, J. B.; Ortiz, J. V.; Cui, Q.; Baboul, A. G.; Clifford, S.; Cioslowski, J.; Stefanov, B. B.; Liu, G.; Liashenko, A.; Piskorz, P.; Komaromi, I.; Martin, R. L.; Fox, D. J.; Keith, T.; Al-Laham, M. A.; Peng, C. Y.; Nanayakkara, A.; Challacombe, M.; Gill, P. M. W.; Johnson, B.; Chen, W.; Wong, M. W.; Gonzalez, C.; Pople, J. A. *Gaussian 03*, revision C.02 ed.; Gaussian, Inc.: Pittsburgh, PA, 2001.
- (45) Amos, R. D.; Bernhardsson, A.; Berning, A.; Celani, P.; Cooper, D. L.; Deegan, M. J. O.; Dobbyn, A. J.; Eckert, F.; Hampel, C.; Hetzer, G.; Knowles, P. J.; Korona, T.; Lindh, R.; Lloyd, A. W.; McNicholas, S. J.; Manby, F. R.; Meyer, W.; Mura, M. E.; Nicklass, A.; Palmieri, P.; Pitzer, R.; Rauhut, G.; Schütz, M.; Schumann, U.; Stoll, H.; Stone, A. J.; Tarroni, R.; Thorsteinsson, T.; Werner, H.-J. MOLPRO, Release 2002.6 ed.
- (46) Gurvich, L. V.; Veyts, I. V.; Alcock, C. B. *Thermodynamic Properties of Individual Substances*, 4th ed.; Hemisphere: New York, 1989.
- (47) Lignell, A.; Lundell, J.; Pettersson, M.; Khriachtchev, L.; Rasanen, M. *Low Temp. Phys.* **2003**, *29*, 844.
- (48) Wang, N. X.; Venkatesh, K.; Wilson, A. K. *J. Chem. Phys. A* **2006**, *110*, 779.
- (49) Wang, N. X.; Wilson, A. K. *J. Chem. Phys.* **2004**, *121*, 7632.
- (50) Wang, N. X.; Wilson, A. K. *Mol. Phys.* **2005**, *103*, 345.
- (51) Bagus, P. S.; Liu, B.; Schaefer, H. F., III. *J. Am. Chem. Soc.* **1972**, *94*, 6635.
- (52) Lignell, A.; Khriachtchev, L.; Lundell, J.; Tanskanen, H.; Rasanen, M. *J. Chem. Phys.* **2006**, *125*, 184514.
- (53) Li, T.-H.; Liu, Y.-L.; Lin, R.-J.; Yeh, T.-Y.; Hu, W.-P. *Chem. Phys. Lett.* **2007**, *434*, 38.
- (54) Howard, W. F.; Andrews, L. *J. Am. Chem. Soc.* **1974**, *96*, 7864.